International Journal of Chemistry Research

Online ISSN- 0976-5689 Vol 8, Issue 3, 2024

Original Article

ISONICOTINOHYDRAZIDE DERIVED SCHIFF BASE–TRANSITION METAL COMPLEXES: STRUCTURE WITH BIOLOGICAL ACTIVITY

AL AKRAMULLAZI, SABIHA SULTANA, FARUK HOSSEN, ALI ASRAF, KUDRAT-E-ZAHAN*

Department of Chemistry, Faculty of Science, Rajshahi University, Rajshahi-6205, Bangladesh
***Corresponding author: Kudrat-E-Zahan; *Email: kudrat.chem@ru.ac.bd**

Received: 10 Apr 2024 Revised and Accepted: 05 Jun 2024

ABSTRACT

Objective: Antimicrobials are medications used for preventing and treating infectious diseases in humans, animals, and plants. Antimicrobial resistance is increasingly becoming a prominent global public health and developmental concern. The primary aim of this study is to synthesize metal complexes with superior antimicrobial properties.

Methods: The Schiff base ligand (E)-N'-(1-thiophen-2-yl) ethylidene isonicotinohydrazide was synthesized by reacting isonicotinohydrazide (INH) with 2-acetylthiophene. This Schiff base was utilized to synthesize metal complexes with copper (II), nickel (II), and cobalt (II) ions via the reflux method. The ligand and metal complexes were characterized using various physicochemical techniques, including elemental analysis, conduct metric studies, magnetic susceptibility, FT-IR, 1H NMR, ESI-MS, and electronic spectral analysis.

Results: All complexes were successfully characterized. The Ni-complex demonstrated the highest cytotoxicity in the brine shrimp lethality bioassay compared to the Cu and Co-complexes. The Ni and Cu-complexes exhibited greater antibacterial efficacy against all bacteria, while the Co-complex showed no activity.

Conclusion: The newly synthesized complexes proved to be highly stable, displaying significant antimicrobial potential. These findings suggest that future modifications to this synthesized series could address specific pharmaceutical needs.

Keywords: Synthesis, Schiff bases, Metal complexes, Characterization, Biological activity

DOI: http://dx.doi.org/10.22159/ijcr.2024v8i3.230 Journal homepage: https://ijcr.info/index.php/journal

INTRODUCTION

Tuberculosis (TB), caused by the pathogenic bacterium *Mycobacterium tuberculosis*, is an extremely severe and deadly infectious disease worldwide [1, 2]. The presence of this infection in individuals with weakened immune systems, particularly those with HIV and severely drug-resistant TB, adds complexity and severity to the disease [3]. Streptomycin and para-aminosalicylic acid were the first antimicrobial treatments for TB in the mid-1940s, but isoniazid (INH) revolutionized treatment in 1952 [4]. Currently, two approaches are being employed to discover novel anti-TB medications. The first approach involves modifying existing anti-TB drugs at the molecular level [5]. The second approach involves testing novel chemicals to determine their effectiveness against M. tuberculosis [6].

Hydrazones (HZN) are a type of chemical molecule containing a>C=N-NH group. They are formed when a ketone or aldehyde reacts with a hydrazine or hydrazide [7]. The structure of HZN exhibits several key features: (i) a nucleophilic imine and an amino-type nitrogen, with the amino-type nitrogen being more reactive; (ii) an imine carbon that possesses both electrophilic and nucleophilic properties; (iii) configurational isomerism resulting from the inherent nature of the>C=N double bond; and (iv) in most cases, an acidic N-H proton. These structural motifs determine the physical and chemical properties of HZN, which are crucial for its applications [8]. Significant attention has been given to acid hydrazides R-CO-NH-NH_2 and their related aryl hydrazones R-CO-NH-N=CH-R due to their interesting biological properties and their ability to bind to transition metal ions found in living organisms [9, 10].

INH is a potent antimicrobial hydrazide specifically designed to eradicate *Mycobacterium tuberculosis*, the causative agent of TB [11]. However, INH has the adverse effect of increasing liver enzyme levels in the bloodstream, which can lead to hepatic damage characterized by cellular necrosis and steatosis. Additionally, the metabolites of this medication can potentially impact liver cells adversely [12]. Therefore, enhancing the therapeutic efficacy of INH, a prominent first-line anti-TB medication, through structural modifications has received significant attention over the years. The methods employed involve creating and evaluating modified versions of INH by adding substituents that either remove or donate electrons to the isonicotinic ring [13]. It has been reported that INH Schiff base (INH SB) possesses superior antitubercular and anticancer activities compared to INH alone [14]. Scientists have explored metal complexes of organic pharmaceuticals as potentially more active than the original organic component, leading them to investigate metal complexes of INH as potential anti-TB drugs [15]. Additionally, isonicotinoylhydrazones and molecules that coordinate with them exhibit remarkable antimicrobial, antifungal, anticancer, antioxidant, and anticonvulsant effects [16].

Considering all of these factors, our objective was to develop a promising ligand and studying the antibacterial, anticancer, and anti-TB properties of a new ligand called isonicotinoylhydrazone and its transition metal complexes [17]

MATERIELS AND METHODS

Instrumentation

Carbon, hydrogen, nitrogen, and sulfur quantities were determined via a PerkinElmer PE 2400 elementary analyzer. The model AZ6512 electrothermal melting point device examined the ligand and metal complexes' melting points. The molar conductivity of complexes in dimethyl sulfoxide (DMSO) has been evaluated with the analyzer CONSORT-C86 for solutions with an average concentration of 10^{-3} M. Using a Bruker Tensor 37 spectrometer, KBr pellets were evaluated with infrared spectra in the 400–4000 cm^{-1} region. A Jasco V670 spectrophotometer recorded

electrical spectra at 200 and 800 nm using the diffuse light reflection method, and Spectral was given as a standard [18]. Employing a Gouy balance, the complexes' magnetic susceptibility was assessed at the ambient temperature [19]. The spectrum of NMR was taken on a Bruker advance detector at 500 MHz for ^{1}H [20]. ESI-MS spectra were done with an Agilent Technologies MSD SL Trap mass spectrometer with an ESI source coupled with an 1100 Series HPLC system.

Materials and reagents

The reagents used in this study, such as Inh, acetyl-2-thiophene, $Co(CH_3COO)_2.4H_2O$, $Cu(CH_3COO)_2$. H_2O and $Ni(CH_3COO)_2.4H_2O$, absolute ethanol, methanol and DMSO were purchased from Aldrich.

Synthesis of ligand and its metal complexes

The synthesis of SB ligand [(E)-N'-(1-(thiophen-2-yl)ethylidene)isonicotinohydrazide]

The ligand (L) was prepared by combining 10 mmol of 2-acetylthiophene (1.26g) with 10 mmol of INH (1.37g) in a round-bottom flask through a condensation reaction. The INH was dissolved in 20 ml of heated ethanol, while 2-acetylthiophene was also dissolved in ethanol. The solutions were then combined and subjected to reflux for 4-5 hours [21]. After cooling, a white crystalline substance was obtained. The product was purified using acetone and diethyl ether and then dried under a pressurized desiccator containing anhydrous $CaCl_2$. The growth and purity of the ligand were assessed by TLC using various solvents. The product yielded 81% and exhibited a yellow color, indicating its solubility in several solvents such as CH_3OH, C_2H_5OH, CCl_4, and DMSO.

Molecular formula: $C_{12}H_{11}ON_3S$; appearance: white crystalline powder; yield: 83%; melting point: 232-234° C; ^{1}H-NMR (400 MHz, DMSO-d^6) δ: 11.0 (-CO-NH, 1H, s), 2.45 (DMSO, 6H, s), 7.10–8.73 (Ar, 7H, m), 2.35 (-CH_3, 3H, s); FT-IR (KBr pellet): ν(-OH)-3400 cm^{-1}, ν(>C=O)-1668 cm^{-1}, ν(>C=N)-1596 cm^{-1}; UV/Vis. (DMSO): λ_{max} at: 267 nm and 324 nm; Ana Cal: C-58.77, H-4.49, N-17.14, S-13.06 Found: C-58.70, H-4.54, N-17.21, S-13.01.

Synthesis of metal complexes

Co-complex: Appearance: light yellow; yield: 67%; melting point:>300° C; molecular formula: $CoC_{24}H_{20}O_2N_6S_2$; conductivity: 3 Sm^2 mol^{-1}; μ_{eff} B. M.: 4.32; FT-IR (KBr pellet): ν(-OH)-3432 cm^{-1}, ν(C–O)-1299 cm^{-1}, ν(>C=N)-1577 cm^{-1}, ν(Co–O)-637 cm^{-1}, ν(Co–N)-481 cm^{-1}; UV/Vis. (DMSO): λ_{max} at: 278 nm and 364 nm; Ana Cal: C-52.66, H-3.66, N-15.36, S-11.70; Found: C-52.70, H-3.61, N-15.41, S-11.64.

Ni-complex: Appearance: yellowish green; yield: 61%; melting point:>300° C; molecular formula: $NiC_{24}H_{20}O_2N_6S_2$; conductivity: 6 Sm^2 mol^{-1}; μ_{eff} B. M.: 2.87; FT-IR (KBr pellet): ν(-OH)-3393 cm^{-1}, ν(C–O)-1302 cm^{-1}, ν(>C=N)-1575 cm^{-1}, ν(Ni–O)-640 cm^{-1}, ν(Ni–N)-476 cm^{-1}; UV/Vis. (DMSO): λ_{max} at 300 nm, 366 nm, and 400 nm; Ana Cal: C-52.68, H-3.66, N-15.36, S-11.71; Found: C-52.64, H-3.71, N-15.41, S-11.62.

Cu-complex: Appearance: light green; yield: 57%; melting point:>300° C; molecular formula: $CuC_{24}H_{20}O_2N_6S_2$; conductivity: 4 Sm^2 mol^{-1}; μ_{eff} B. M.: 1.85; FT-IR (KBr pellet): ν(-OH)-3424 cm^{-1}, ν(C–O)-1305 cm^{-1}, ν(>C=N)-1577 cm^{-1}, ν(Cu–O)-638 cm^{-1}, ν(Cu–N)-458 cm^{-1}; UV/Vis. (DMSO): λ_{max} at 262 nm, 290 nm, and 418 nm; Ana Cal: C-52.22, H-3.63, N-15.23, S-11.60; Found: C-52.15, H-3.69, N-15.17, S-11.64.

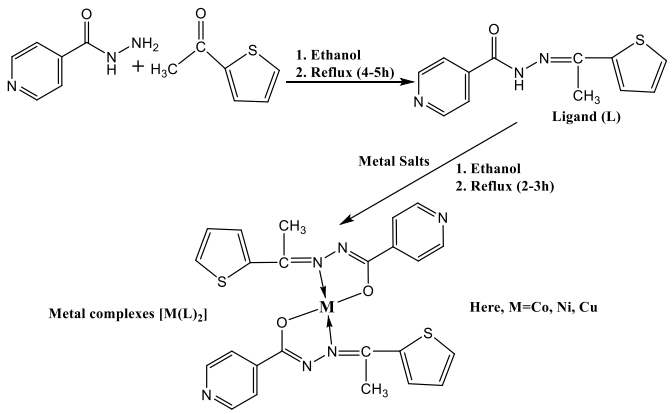

Fig. 1: Synthetic pathway for the formation of l and its metal complexes

RESULTS AND DISCUSSION

Elemental and molar conductivity studies

The metal percentage was determined using complexometric titration with EDTA, following the procedure outlined in the literature [23]. Table 1 presents the analytical data for the percentages of M (II), C, H, N, and S in the complexes, both observed and calculated. The molar conductivities were measured at a concentration of 10-3M in DMSO at ambient temperature table 1. The lower conductance level confirms the non-electrolytic nature of the complexes [24].

Table 1: Physical-chemical and analytical data on SB ligand and its complexes with metals

Compounds	Empirical formula	Elemental analysis found (cal) (%)					Λ^a
		C	H	N	S	M	Sm^2 mol^{-1}
L	$C_{12}H_{11}ON_3S$	58.70(58.77)	4.54(4.49)	17.21(17.14)	13.01(13.06)	----	----
Ni-complex	$NiC_{24}H_{20}O_2N_6S_2$	52.64(52.68)	3.71(3.66)	15.41(15.36)	11.62(11.71)	10.70(10.74)	6
Co-complex	$CoC_{24}H_{20}O_2N_6S_2$	52.70(52.66)	3.61(3.66)	15.41(15.36)	11.64(11.70)	10.82(10.77)	3
Cu-complex	$CuC_{24}H_{20}O_2N_6S_2$	52.15(55.22)	3.69(3.63)	15.17(15.23)	11.64(11.60)	11.56(11.51)	4

FT-IR spectra

The spectra of the ligand (L), Co-complex, Ni-complex, and Cu-complex can be observed in fig. 2. These spectra were obtained using the Fourier transform infrared (FT-IR) method. The stretching frequencies of the ν(-OH), ν(-NH), and ν(-CH) groups were determined by assigning absorption bands at wavenumbers of 3400 cm^{-1}, 3180 cm^{-1}, and 3034 cm^{-1}, respectively. Additionally, peaks at 1596 cm^{-1} and 1668 cm^{-1} correspond to vibrational modes of the ν(C=N) and ν(C=O) functional groups [25]. In the FT-IR spectra of the metal complexes, the band of the l ligand shifted from 1596 cm^{-1} to 1577 cm^{-1}, 1575 cm^{-1}, and 1577 cm^{-1} for the Co-complex, Ni-complex, and Cu-complex, respectively, due to the azomethine moiety (>C=N). This shift indicates coordination of the metal ion with the N-atom of the (>C=N) group. Furthermore, the stretching frequency of the ligand's (>C=O) group at 1668 cm^{-1} shifted to 1299 cm^{-1}, 1302 cm^{-1}, and 1305 cm^{-1} in the Co-complex, Ni-complex, and Cu-complex, respectively, indicating the influence of oxygen on coordination. The appearance of new bond stretching frequencies at 640 cm^{-1}, 638 cm^{-1}, and 637 cm^{-1} suggests the formation of Ni-O, Cu-O, and Co-O bonds, while frequencies at 476 cm^{-1}, 458 cm^{-1}, and 481 cm^{-1} indicate Ni-N, Cu-N, and Co-N bonds, respectively. Additionally, a significant peak observed between 3350 and 3450 cm^{-1} in the IR spectra of the Co-complex, Ni-complex, and Cu-complex complexes is likely due to water present in the KBr pellet [26]. Table 2 presents the FT-IR spectral data of the ligand (L) and its Co(II), Ni(II), and Cu(II) metal complexes.

Table 2: The l and its Co (II), Ni (II), and Cu (II) metal complex FT-IR spectrum data (in cm^{-1})

Compounds	ν(-OH)	ν(>C=N)	ν(>C=O)	ν(C–O)	ν(M–O)	ν(M–N)
L	3400	1596	1668	----	----	----
Ni-complex	3393	1575	----	1302	640	476
Cu-complex	3424	1577	----	1305	638	458
Co-complex	3432	1577	----	1299	637	481

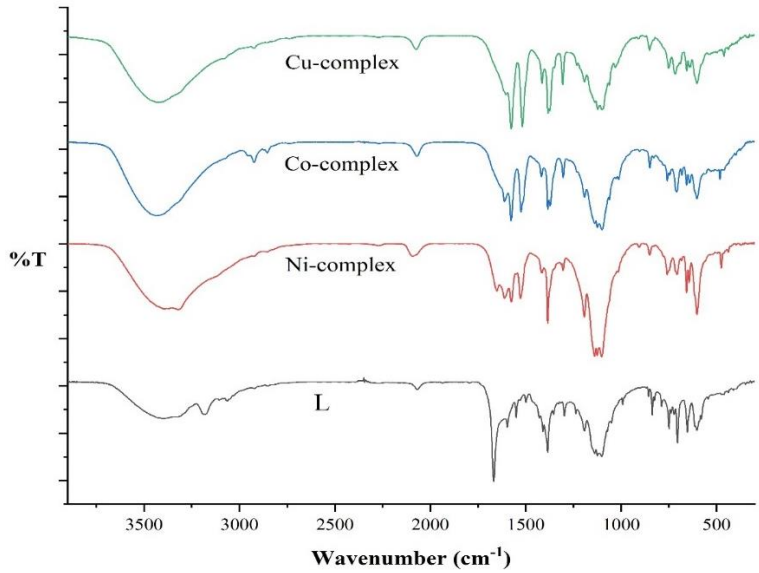

Fig. 2: FT-IR spectra of l and its metal complexes

UV-Vis spectra

The ligand (L) and its Ni(II), Cu(II), and Co(II) metal complexes in DMSO were analyzed by electronic spectroscopy, and the spectral data are presented in table 3. The visible and ultraviolet spectra exhibited numerous intense absorption bands for both the ligands and complexes. Electronic spectra of both the ligand (L) and the complexes were obtained after dissolving them in DMSO at room temperature. In the electronic spectra of the ligand (L), strong absorption peaks at 267 nm and 324 nm are observed. Fig. 3 illustrates that these peaks are attributed to π→π* and n→π* transitions.

As depicted in fig. 3, the Ni-complex exhibited three UV-Vis absorption bands at 300 nm, 366 nm, and 400 nm. Changes in the electronic spectra of the ligand (L) at 267 nm and 324 nm were observed upon binding to Ni(II) ions in this experiment, indicating l's interaction with Ni(II) ions.

The absorption peak at 300 nm was attributed to the π→π* transition, while the peak at 366 nm was attributed to the n→π* transition, which arise from the unshared pair of electrons on the azomethine nitrogen and an antibonding p orbital. Fig. 3 also illustrates a 400 nm absorption band corresponding to the l-to-metal charge transfer.

The Cu-complex exhibits three UV-Vis absorption bands at 262 nm, 290 nm, and 418 nm, as depicted in fig. 3. The electronic spectra of the ligand (L) at 267 nm and 324 nm were altered by the Cu-complex, indicating interaction between l and Cu(II) ions. The absorption at 262 nm corresponds to the π→π* transition, while the absorption at 290 nm is attributed to the n→π* transition, which is induced by the lone electron pair on the azomethine nitrogen and the antibonding p orbital. Additionally, the absorption band at 418 nm in fig. 3 demonstrates charge transfer from l to the metal.

The Co-complex displays three UV-Vis absorption bands at 278 nm and 364 nm. The peak at 278 nm is assigned to the π→π* transition, which occurs due to the lone electron pair on the azomethine nitrogen and the antibonding p orbital. At 364 nm, fig. 3 illustrates charge transfer from l to the metal in the molecule's absorption band.

Based on UV spectral data and magnetic moment values (fig. 4(a, b, c)), the Co, Ni, and Cu complexes are suggested to be tetrahedral [27].

Table 3: Electronic spectrum data and magnetic moments for l and its metal complexes

Compounds	Empirical formula	λ_{max} nm	μ_{eff} B. M	Assignment
L	$C_{12}H_{11}ON_3S$	267	---	π→π*
		324		n→π*
Ni-complex	$[NiC_{24}H_{20}O_2N_6S_2]$	300	2.87	π→π*
		366		n→π*
		400		C. T (L→M)
Cu-complex	$[CuC_{24}H_{20}O_2N_6S_2]$	262	1.85	π→π*
		290		n→π*
		418		C. T (L→M)
Co-complex	$[CoC_{24}H_{20}O_2N_6S_2]$	278	4.32	π→π*
		364		C. T (L→M)

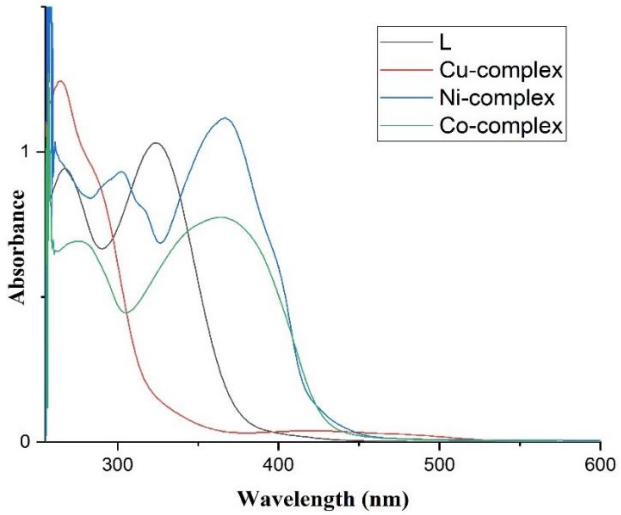

Fig. 3: Electronic spectra of l and its metal complexes

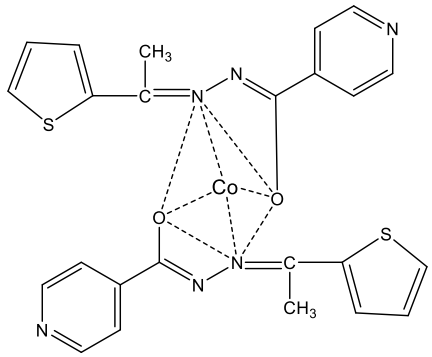

Fig. 4(a): Proposed structure of $[CoC_{24}H_{20}O_2N_6S_2]$ complex (Tetrahedral)

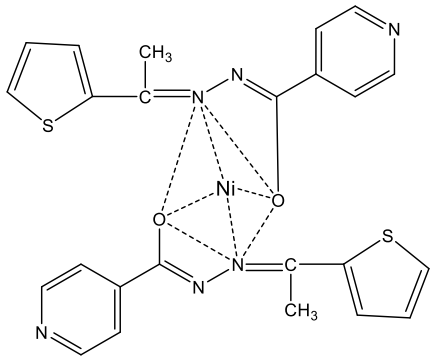

Fig. 4(b): Proposed structure of $[NiC_{24}H_{20}O_2N_6S_2]$ complex (Tetrahedral)

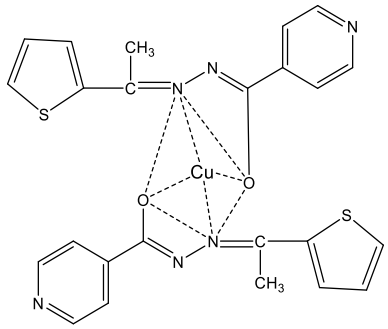

Fig. 4(c): Proposed structure of [$CuC_{24}H_{20}O_2N_6S_2$] complex (Tetrahedral)

^{1}H-NMR spectroscopy

Fig. 5 displays the ^{1}H-NMR spectra of the ligand (L) after dissolution in DMSO [28]. The prominent peak at a chemical shift of 2.3 ppm corresponds to the proton of the-CH_3 group. The protons of the pyridine and thiophene rings appear as two doublet signals within a chemical shift range of 7.1–8.7 ppm. The proton of the amide CO-NH, which is highly acidic, appears as a singlet at a chemical shift of 11.0 ppm [29].

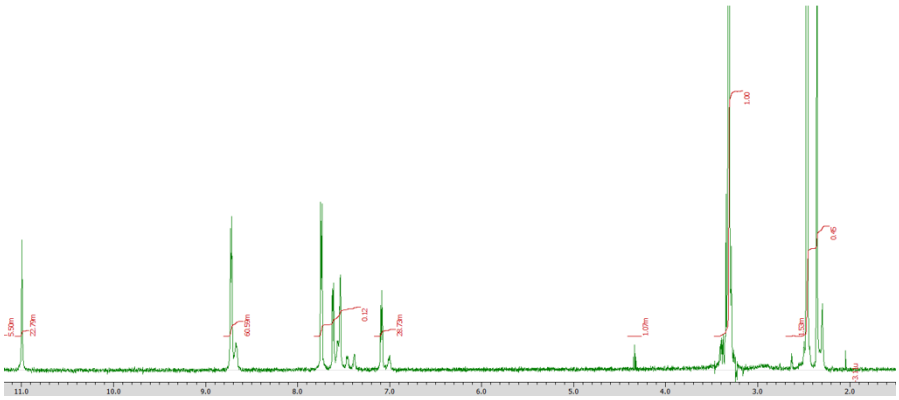

Fig. 5: ^{1}H-NMR spectra of l delta value (ppm)

ESI-mass spectral investigations of the l and Its complexes with Co (II), Ni (II), and Cu (II) Ions

The ESI-MS spectra of the investigated l showed the presence of a most abundant signal at *m/z* = 246.4718 ([L+H]$^+$) corresponding to the protonated molecular ion of the l, and less abundant signals at *m/z* = 79.5783 and 86.5301, corresponding to the two aromatic rings detached from the protonated l. The ESI-MS spectra of the synthesized metal complexes in slightly acidified DMSO reveal that these complexes show several fragmentations. The ESI-MS spectra display the most abundant peaks at *m/z* = 547.4078, 548.8765, and 553.1634, corresponding to the intact molecular ions for Co-complex, Ni-complex, and Cu-complex, respectively (fig. 6).

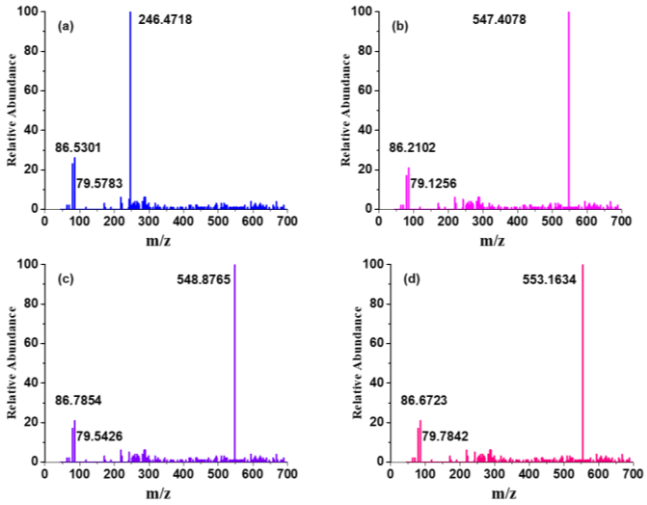

Fig. 6: The ESI-MS spectra of (a) l, (b) Co-complex, (c) Ni-complex, and (d) Cu-complex

Microbiological evaluation

The global prevalence of antimicrobial drug-resistant bacteria is rapidly increasing, leading to a progressive decline in the effectiveness of antibiotics [30]. Antimicrobial resistance (AMR) poses a widely recognized threat to public health. The emergence and global spread of novel resistance mechanisms are jeopardizing our ability to effectively combat infectious diseases, particularly in developing nations where second-and third-line medicines are not readily accessible or affordable.

This study investigated the antibacterial properties of the ligand (L) and its metal complexes against Pseudomonas aeruginosa, Escherichia coli, Staphylococcus aureus, and Bacillus cereus. The diameter of the inhibitory zones was measured in millimeters, and the results were compared with standard Kanamycin-30. The findings of their antibacterial activity are reported in table 4 (fig. 7) [31]. The Ni and Cu-complexes exhibited greater antibacterial efficacy against all bacteria compared to the unbound l, while the Co-complex showed no activity. Among all synthesized compounds, the Ni-complex displayed significant antibacterial activity against Pseudomonas aeruginosa, whereas the Cu-complex exhibited superior activity against Escherichia coli, Staphylococcus aureus, and Bacillus cereus.

The enhanced antibacterial efficacy of metal complexes compared to the unbound ligand can be comprehensively explained by Overtone's concept and Tweedy's chelation hypothesis [32]. Chelation with l reduces the polarity of a metal ion because the positive charge of the metal ion is partially shared with donor groups (such as O, N, S, etc., depending on the ligand's structure). Additionally, there is potential for π-electron delocalization within the chelate ring. Chelation with l significantly increases the lipophilicity of the central metal ion, facilitating its passage through the lipid layers of the cell membrane and preventing it from binding to metal-binding sites on microbial enzymes [33, 34].

The effectiveness of different chemicals against specific species is influenced by the impermeability of microorganisms' cell membranes or alterations in the ribosomes of microbial cells. The fig. and tables presented below display the outcomes of the antibacterial activity of different samples against harmful bacteria [35].

Table 4: Antibacterial activities (zone of inhibition in mm) of samples against pathogens

Samples	*Pseudomonas aeruginosa*	*Escherichia coli*	*Bacillus cereus*	*Staphylococcus aureus*
Kanamycin-30	27	24	25	26
L	11	10	10	12
Cu-complex	0	14	14	14
Ni-complex	15	12	12	13
Co-complex	0	0	0	0

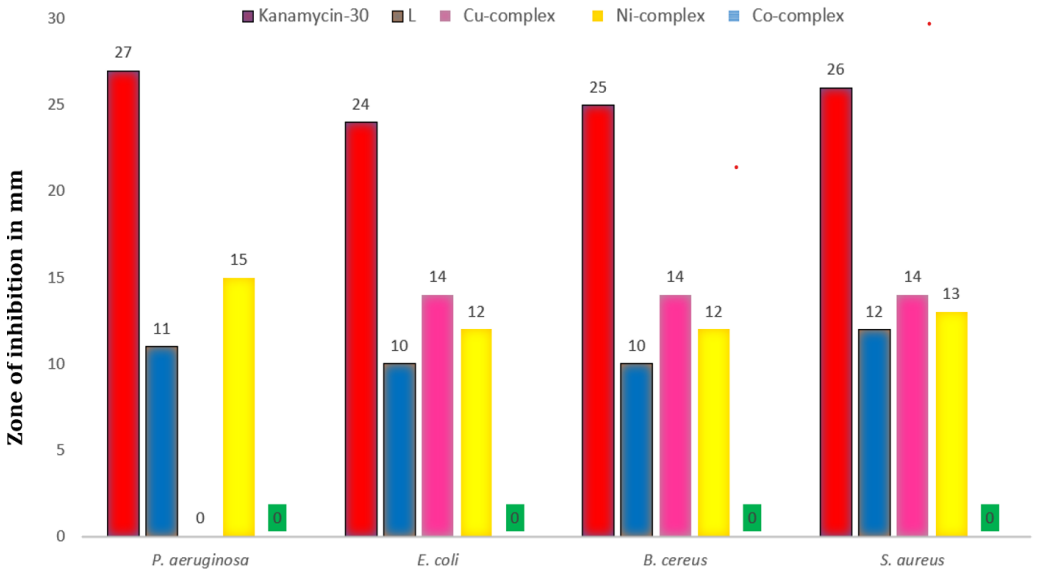

Fig. 7: Zone of inhibition of samples and standard against Pseudomonas aeruginosa, Escherichia coli, Staphylococcus aureus, Bacillus cereus. Data is expressed as mean of three determinations.

Cytotoxicity evaluation

The brine shrimp lethality bioassay is employed to quickly and easily evaluate the cytotoxicity of bioactive compounds [36]. The lethality test conducted on brine shrimp revealed that the ligand (L) and its metal compounds exhibit significant activity, as shown in table 5 (fig. 8). According to the current experiment, there is a direct correlation between the concentrations of the compounds and the degree of lethality. The concentration of 100 µg/ml resulted in the highest fatality rates, while the concentration of 6.25 µg/ml showed the lowest death rates, as indicated in table 5 [37].

All the produced compounds demonstrated positive results in the brine shrimp lethality test, confirming their biological activity. Among these, the Ni-complex exhibited enhanced cytotoxicity with lC50 values of 17.64 µg/ml compared to l and other complexes when compared to the conventional vincristine sulfate, which had an lC50 of 12.09 µg/ml [38]. It is speculated that the Ni-complex may possess cytotoxic or anticancer properties. Subsequently, in vivo experiments will be conducted to assess whether the substances harm or selectively target cancer cells. We recommend utilizing a zebrafish animal model for this purpose [39].

Table 5: Brine Shrimp lethality Bioassay

Sample	Conc. of the Sample (µg/ml)	Log conc. (µg/ml)	Number of nauplii used	Number of nauplii survived (After 24h)	Percentage of mortality	Probit value	LC_{50} Value (µg/ml)
Standard	6.25	0.7959	30	23	23	4.26	12.09
(Vincristine	12.5	1.0969	30	14	57	5.18	
sulphate)	25	1.3979	30	10	67	5.44	
	50	1.6990	30	5	83	5.95	
	100	2.0000	30	0	100	8.95	
L	6.25	0.7959	13	9	30.76	4.48	
	12.5	1.0969	13	9	30.76	4.48	26.11±6.15
	25	1.3979	13	8	38.46	4.69	
	50	1.6990	13	5	61.53	5.28	
	100	2.0000	13	1	92.31	6.41	
Ni-complex	6.25	0.7959	14	13	7.14	3.52	
	12.5	1.0969	14	9	35.71	4.61	17.64±0.94
	25	1.3979	14	5	64.28	5.36	
	50	1.6990	14	1	92.85	6.41	
	100	2.0000	14	0	100	8.95	
Cu-complex	6.25	0.7959	13	13	0	0	
	12.5	1.0969	13	9	30.77	4.48	26.84±3.20
	25	1.3979	13	7	46.15	4.90	
	50	1.6990	13	4	69.23	5.50	
	100	2.0000	13	1	92.31	6.41	
Co-complex	6.25	0.7959	14	12	14.29	3.92	
	12.5	1.0969	14	12	14.28	3.92	33.32±4.13
	25	1.3979	14	11	21.41	4.19	
	50	1.6990	14	2	85.71	6.04	
	100	2.0000	14	1	92.85	6.41	

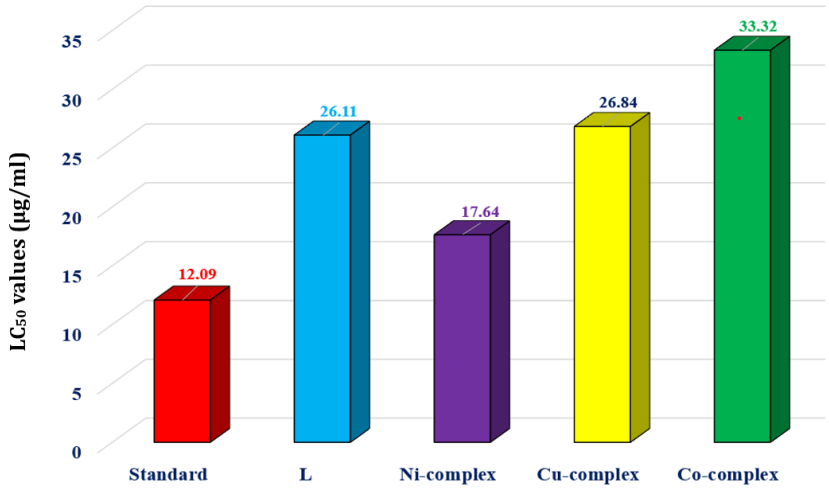

Fig. 8: LC_{50} values of sample and standard

CONCLUSION

Metal complexes with Co(II), Ni(II), and Cu(II) ions were synthesized using the resynthesized ligand (L) (E)-N'-(1-(thiophen-2-yl)ethylidene) isonicotinohydrazide. The ligand (L) and its metal complexes were analyzed using TLC, melting point determination, conductivity testing, magnetic moment measurement, FT-IR spectroscopy, 1H-NMR spectroscopy, ESI-MS, and UV-Vis spectroscopy. Conductivity tests of the complexes indicated that all of them are non-electrolytes when dissolved in liquids. FT-IR spectra observed in the infrared spectrum show that the ligand functions as a chelate through the nitrogen and oxygen atoms that make up the hydrazone group. Complexes exhibit tetrahedral stereochemistry based on UV-Vis and magnetic susceptibility measurements.

The ligand (L) and its metal complexes exhibited biological activity and were cytotoxic to brine shrimp nauplii. The Ni-complex showed higher cytotoxic activity. The ligand (L) and its complexes were also tested for antibacterial action against certain microbes. The Ni-complex exhibited higher antibacterial activity compared to the ligand alone. Therefore, the cytotoxic activity data of these ligands and their metal complexes demonstrate their potential as promising anticancer molecules. Moreover, these findings suggest new possibilities for future modifications in the synthesized series to meet pharmaceutical needs.

ACKNOWLEDGMENT

The authors appreciate Chairman, Department of Chemistry, University of Rajshahi, Bangladesh, for supplying the laboratory resources.

FUNDING

Nil

AUTHORS CONTRIBUTIONS

Al Akramullazi and Mst. Sabiha Sultana researched literature, conceived the study and wrote the first draft of the manuscript. Md. Faruk Hossen and Md. Ali Asraf involved in data analysis. Md. Kudrat-E-Zahan supervised the overall work. All authors reviewed and edited the manuscript and approved the final version of the manuscript.

CONFLICT OF INTERESTS

Declared none

REFERENCES

1. More G, Bootwala S, Shenoy S, Mascarenhas J, Aruna K. Synthesis, characterization and *in vitro* antitubercular and antimicrobial activities of new aminothiophene schiff bases and their Co(II), Ni(II), Cu(II) and Zn(II) metal complexes. Orient J Chem. 2018;34(2):800-12. doi: 10.13005/ojc/340225.
2. Nazim U, Ali SI, Ishrat G, Hassan A, Ahmed M, Ali M. Synthesis, characterization and SEM studies of novel 1-indanyl isoniazid and hydrazide Schiff base derivatives as new anti-tubercular agents. Pak J Pharm Sci. 2020;33(3):1095-103. doi: 10.36721/PJPS.2020.33.3, PMID 33191234.
3. Dueke Eze CU, Fasina TM, Oluwalana AE, Familoni OB, Mphalele JM, Onubuogu C. Synthesis and biological evaluation of copper and cobalt complexes of (5-substituted-salicylidene) isonicotinichydrazide derivatives as antitubercular agents. Sci Afr. 2020;9:e00522. doi: 10.1016/j.sciaf.2020.e00522.
4. Judge V, Narasimhan B, Ahuja M. Isoniazid: the magic molecule. Med Chem Res. 2012;21(12):3940-57. doi: 10.1007/s00044-011-9948-y.
5. Quan D, Nagalingam G, Payne R, Triccas JA. New tuberculosis drug leads from naturally occurring compounds. Int J Infect Dis. 2017;56:212-20. doi: 10.1016/j.ijid.2016.12.024, PMID 28062229.
6. Kotapalli SS, Nallam SS, Nadella L, Banerjee T, Rode HB, Mainkar PS. Identification of new molecular entities (NMEs) as potential leads against tuberculosis from open-source compound repository. Plos One. 2015;10(12):e0144018. doi: 10.1371/journal.pone.0144018, PMID 26642200.
7. Jeyaraman P, Alagarraj A, Natarajan R. In silico and *in vitro* studies of transition metal complexes derived from curcumin–isoniazid Schiff base. J Biomol Struct Dyn. 2020;38(2):488-99. doi: 10.1080/07391102.2019.1581090, PMID 30767624.
8. Ferraresi Curotto V, Echeverría GA, Piro OE, Pis-Diez R, Gonzalez Baro AC. Synthesis and characterization of a series of isoniazid hydrazones. Spectroscopic and theoretical study. J Mol Struct. 2017;1133:436-47. doi: 10.1016/j.molstruc.2016.12.018.
9. Aggarwal RC, Singh NK, Singh RP. Synthesis and structural studies of some first-row transition metal complexes of salicylaldehyde hydrazone. Inorg Chim Acta. 1979;32:L87-90. doi: 10.1016/S0020-1693(00)91625-6.
10. Anten JA, Nicholls D, Markopoulos JM, Markopoulou O. Transition-metal complexes of hydrazones derived from 1,4-diformyl- and 1,4-diacetylbenzenes. Polyhedron. 1987;6(5):1075-80. doi: 10.1016/S0277-5387(00)80958-4.
11. Hunoor RS, Patil BR, Badiger DS, Vadavi RS, Gudasi KB, Chandrashekhar VM. Spectroscopic, magnetic and thermal studies of Co(II), Ni(II), Cu(II) and Zn(II) complexes of 3-acetylcoumarin-isonicotinoylhydrazone and their antimicrobial and anti-tubercular activity evaluation. Spectrochim Acta A Mol Biomol Spectrosc. 2010;77(4):838-44. doi: 10.1016/j.saa.2010.08.015, PMID 20833102.
12. Ramya Rajan MP, Rathikha R, Nithyabalaji R, Sribalan R. Synthesis, characterization, in silico studies and *in vitro* biological evaluation of isoniazid-hydrazone complexes. J Mol Struct. 2020;1216. doi: 10.1016/j.molstruc.2020.128297.
13. Dueke Eze CU, Fasina TM, Oluwalana AE, Familoni OB, Mphalele JM, Onubuogu C. Synthesis and biological evaluation of copper and cobalt complexes of (5-substituted-salicylidene) isonicotinichydrazide derivatives as antitubercular agents. Sci Afr. 2020;9:e00522. doi: 10.1016/j.sciaf.2020.e00522.
14. Sharma KK, Singh R, Fahmi N, Singh RV. Synthesis, coordination behavior, and investigations of pharmacological effects of some transition metal complexes with isoniazid schiff bases. J Coord Chem. 2010;63(17):3071-82. doi: 10.1080/00958972.2010.504986.
15. Silva PB, Souza PC, Calixto GM, Lopes Ede O, Frem RC, Netto AV. *In vitro* activity of copper (II) complexes, loaded or unloaded into a nanostructured lipid system, against mycobacterium tuberculosis. Int J Mol Sci. 2016;17(5). doi: 10.3390/ijms17050745, PMID 27196901.
16. Trzesowska Kruszynska A. Solvent-free and catalysis-free approach to the solid state in situ growth of crystalline isoniazid hydrazones. Cryst Growth Des. 2013;13(9):3892-900. doi: 10.1021/cg400529s.
17. Hunoor RS, Patil BR, Badiger DS, Vadavi RS, Gudasi KB, Chandrashekhar VM. Spectroscopic, magnetic and thermal studies of Co(II), Ni(II), Cu(II) and Zn(II) complexes of 3-acetylcoumarin-isonicotinoylhydrazone and their antimicrobial and anti-tubercular activity evaluation. Spectrochim Acta A Mol Biomol Spectrosc. 2010;77(4):838-44. doi: 10.1016/j.saa.2010.08.015, PMID 20833102.
18. Zarafu I, Badea M, Ionita G, Chifiriuc MC, Bleotu C, Popa M. Thermal, spectral and biological characterisation of copper(II) complexes with isoniazid-based hydrazones. J Therm Anal Calorim. 2019;136(5):1977-87. doi: 10.1007/s10973-018-7853-z.
19. Kulkarni GS, Anandgaonker PL, Janrao SD, Gaikwad DD, Janrao DM. Synthesis, characterization and biological evaluation of transition metal complexes M(II) derived from n. o bidentate ligands. Int J Mol Sci. 2015 May 15;16(5):11034-54. doi: 10.3390/ijms160511034.
20. Ahmed M, Rooney D, McCann M, Devereux M, Twamley B, Galdino AC, Sangenito lS, Souza lO, lourenço MC, Gomes K, Dos Santos AL. Synthesis and antimicrobial activity of a phenanthroline-isoniazid hybrid ligand and its Ag+and Mn 2+complexes. BioMetals. 2019;32:671-82. doi: 10.1007/s10534-019-00204-5.
21. Trzesowska Kruszynska A. Solvent-free and catalysis-free approach to the solid state in situ growth of crystalline isoniazid hydrazones. Cryst Growth Des. 2013;13(9):3892-900. doi: 10.1021/cg400529s.
22. Camellia FK, Ashrafuzzaman M, Islam MN, Banu LA, Kudrat-E-Zahan M. Synthesis, characterization, antibacterial and antioxidant studies of isoniazid-based Schiff base ligands and their metal complexes. AJACR. 2022;11:8-23. doi: 10.9734/AJACR/2022/v11i330257.
23. Chu LF, Shi Y, Xu DF, Yu H, Lin JR, He QZ. Synthesis and biological studies of some lanthanide complexes of schiff base. Synth React Inorg Metal-Organic Nano-Metal Chem. 2015;45(11):1617-26. doi: 10.1080/15533174.2015.1031048.
24. Kulkarni GS, Anandgaonker PL, Janrao SD, Gaikwad DD, Janrao DM. Synthesis, characterization and biological evaluation of transition metal complexes m (ii). Derived from n, o bidentate ligands. WJPR. 2016;5(4):707-14. doi: 10.20959/wjpr20164-5756.
25. Warad I, Bsharat O, Tabti S, Djedouani A, Al-Nuri M, Al-Zaqri N. Crystal interactions, computational, spectral and thermal analysis of (E)-N'-(thiophen-2-ylmethylene)isonicotinohydrazide as O-N-S-tridentate schiff base ligand. J Mol Struct. 2019;1185:290-9. doi: 10.1016/j.molstruc.2019.02.109.
26. Gordon SH, Mohamed A, Harry-O'Kuru RE, Imam SH. A chemometric method for correcting fourier transform infrared spectra of biomaterials for interference from water in KBr discs. Appl Spectrosc. 2010;64(4):448-57. doi: 10.1366/000370210791114301, PMID 20412631.

27. Ashrafuzzaman MD, Camellia FK, Mahmud AA, Pramanik MJ, Nahar K, Haque MM. Bioactive mixed ligand metal complexes of Cu(II), Ni(II), and Zn(II) ions: synthesis, characterization, antimicrobial and antioxidant properties. J Chil Chem Soc. 2021;66(3):5295-9. doi: 10.4067/S0717-97072021000305295.
28. Ahamad T, Nishat N, Parveen S. Synthesis, characterization and anti-microbial studies of a newly developed polymeric Schiff base and its metal-poly chelates. J Coord Chem. 2008;61(12):1963-72. doi: 10.1080/00958970701795698.
29. Warad I, Bsharat O, Tabti S, Djedouani A, Al-Nuri M, Al-Zaqri N. Crystal interactions, computational, spectral and thermal analysis of (E)-N'-(thiophen-2-ylmethylene)isonicotinohydrazide as O-N-S-tridentate schiff base ligand. J Mol Struct. 2019;1185:290-9. doi: 10.1016/j.molstruc.2019.02.109.
30. Baluja S, Solanki A, Kachhadia N. Evaluation of biological activities of some Schiff bases and metal complexes. J Iran Chem Soc. 2006;3(4):312-7. doi: 10.1007/BF03245952.
31. Zarafu I, Badea M, Ionita G, Chifiriuc MC, Bleotu C, Popa M. Thermal, spectral and biological characterisation of copper(II) complexes with isoniazid-based hydrazones. J Therm Anal Calorim. 2019;136(5):1977-87. doi: 10.1007/s10973-018-7853-z.
32. Camellia FK, Ashrafuzzaman M, Islam MN, Banu LA, Kudrat-E-Zahan M. Synthesis, characterization, antibacterial and antioxidant studies of isoniazid-based Schiff base ligands and their metal complexes. AJACR. 2022;11:8-23. doi: 10.9734/AJACR/2022/v11i330257.
33. Chu LF, Shi Y, Xu DF, Yu H, Lin JR, He QZ. Synthesis and biological studies of some lanthanide complexes of schiff base. Synth React Inorg Metal-Organic Nano-Metal Chem. 2015;45(11):1617-26. doi: 10.1080/15533174.2015.1031048.
34. Ahamad T, Nishat N, Parveen S. Synthesis, characterization and anti-microbial studies of a newly developed polymeric Schiff base and its metal-poly chelates. J Coord Chem. 2008;61(12):1963-72. doi: 10.1080/00958970701795698.
35. Song B, Yang S, Hong Y, Zhang G, Jin L, Hu D. Synthesis and bioactivity of fluorine compounds containing isoxazolylamino and phosphonate groups. J Fluor Chem. 2005;126(9-10):1419-24. doi: 10.1016/j.jfluchem.2005.08.005.
36. Tawaha KA. Cytotoxicity evaluation of Jordanian wild plants using brine shrimp lethality test. Jordan J Appl Sci Nat Sci. 2006;8(1):12.
37. Alam MS, Lee DU, Bari ML. Antibacterial and cytotoxic activities of schiff base analogues of 4-aminoantipyrine. J Korean Soc Appl Biol Chem. 2014;57(5):613-9. doi: 10.1007/s13765-014-4201-2.
38. Patel MN, Patel CR, Joshi HN. Synthesis, characterization and biological studies of mononuclear copper(II) complexes with ciprofloxacin and N, O donor ligands. Inorg Chem Commun. 2013;27:51-5. doi: 10.1016/j.inoche.2012.10.018.
39. Padmaja R, Arun PC, Prashanth D, Deepak M, Amit A, Anjana M. Brine shrimp lethality bioassay of selected Indian medicinal plants. Fitoterapia. 2002;73(6):508-10. doi: 10.1016/S0367-326X(02)00182-X, PMID 12385875.